

## Photon channelling in foams

A. S. GITTINGS, R. BANDYOPADHYAY and D. J. DURIAN

*UCLA Department of Physics and Astronomy - Los Angeles, CA 90095-1547, USA*

(received 19 August 2003; accepted in final form 12 November 2003)

PACS. 82.70.Rr – Aerosols and foams.

PACS. 42.68.Ay – Propagation, transmission, attenuation, and radiative transfer.

**Abstract.** – We report on the absorption of diffuse photons in aqueous foams by a dye added to the continuous liquid phase. For very wet and for dry foams, the absorption of the diffuse photons equals the absorption length of the liquid divided by the liquid volume fraction. This indicates that the diffuse photons propagate by a random walk, sampling each phase in proportion to its volume. Foams of intermediate wetness, by contrast, absorb photons more strongly than expected. A 2D computer simulation, modeling photons scattering in a foam crystal, also shows enhanced absorption. This encourages us to consider novel transport effects, such as the total internal reflection of photons inside the Plateau borders.

Aqueous foams are composed of gas bubbles dispersed in a network of surfactant solution [1]. Even though both components are clear, bulk foams are opaque due to reflection/refraction at the liquid/gas interfaces. This hampers imaging, but opens the possibility of multiple-light scattering techniques [2–4]. Diffuse-transmission spectroscopy (DTS) [5] and diffusing-wave spectroscopy (DWS) [6,7] provide noninvasive probes of structure and dynamics, respectively, in bulk samples. A key parameter is the photon transport mean free path,  $l^*$ , defined by the photon diffusion coefficient,  $cl^*/3$ . Intuitively,  $l^*$  is the distance over which the photon direction becomes randomized. For foams, experiments show that  $l^*$  is proportional to the average bubble diameter [2],  $D$ , with a coefficient that depends on the liquid volume fraction,  $\varepsilon$ . The empirical form

$$l^* \approx D(0.14/\varepsilon + 1.5) \quad (1)$$

was observed for  $0.008 < \varepsilon < 0.3$ , a range of bubble sizes, and two different foaming solutions [8]. This quantifies how wetter foams with smaller bubbles have a shorter transport mean free path and a more opaque appearance.

A key challenge is to relate  $l^*$  to the detailed microstructure of the foam. For dry foams, there are three distinct structural elements: thin soap films separating neighboring bubbles; Plateau borders, at which three films meet; and vertices, at which four Plateau borders meet. The borders and vertices inflate as the liquid fraction,  $\varepsilon$ , increases [1,9]. The film thickness is constant, independent of  $\varepsilon$ . For typical foams, where the film thickness is much smaller than the border thickness and where the border thickness, in turn, is much smaller than the bubble diameter, most of the liquid resides in the borders. Therefore, one might expect that most of the light scattering be due to the Plateau borders. The value of  $l^*$  should then scale as the

reciprocal of the product of the number density and geometrical cross-section of the Plateau borders:  $l^* \propto D/\sqrt{\varepsilon}$ . However, data rule out this form in favor of eq. (1). This may imply significant scattering occurs from vertices [10] or films [11]. It may also imply that photons do not perform a truly random walk; for example, the average propagation direction could be correlated with the local structure.

In this paper, we gauge the extent to which photons execute a random walk through foams in terms of the fraction  $f$  of a photon's path that lies in the liquid phase. A result of  $f = \varepsilon$  means the walk is truly random, with photons sampling the two phases in proportion to their volumes. To deduce the value of  $f$ , we measure the absorption length  $l_a$  of the foam as a function of the absorption length  $l_a^{\text{soln}}$  of the liquid solution. If a photon path has length  $s$ , then the length in the liquid is  $fs$  and the survival probability for a photon travelling that path is  $\exp[-(fs)/l_a^{\text{soln}}] = \exp[-s/l_a]$ . Hence the absorption length of the foam is

$$l_a = l_a^{\text{soln}}/f. \quad (2)$$

To begin, we describe procedures for creating foams and measuring their absorption lengths. Then we analyze our results in terms of both  $f$  and the average transmission probabilities for photons to cross from liquid to gas and vice versa. Finally, we compare with a computer simulation of photon propagation inside an idealized foam structure.

*Procedures.* – Aqueous foam is produced by turbulent mixing [12] of  $\text{N}_2$  gas with a jet of  $\alpha$ -olephinsulphonate (AOS) plus rhodamine solution. By changing the ratio of the gas to liquid flow rates, we generate foams of liquid fractions in the range  $0.03 \leq \varepsilon \leq 0.35$ . The average bubble diameter depends on the foam liquid fraction and is  $100 \mu\text{m}$  for the wettest foam and  $300 \mu\text{m}$  for the driest foam. The foam is loaded *in situ* in a polycarbonate cell of thickness  $L$ .  $L$  may be varied by compressing the closed-cell polyurethane foam gasket between the two polycarbonate plates. The liquid fraction is calculated by weighing the foam that comes out of the outlet hose of the foam cell; it is reproducible to 1%.

The absorptivity of the foam is controlled by adding rhodamine dye to the surfactant solution. The absorption length of the solution ( $l_a^{\text{soln}}$ ) is estimated from ballistic transmission experiments through the rhodamine solutions, using  $T_b = \exp[-L/l_a^{\text{soln}}]$ . The results are accurately described by  $l_a^{\text{soln}} = (0.44 \text{ cm-g/l})/[\text{R}]$ , where  $[\text{R}]$  is the rhodamine concentration.

The absorption optics of foams is studied in terms of the probability  $T_d$  for an incident photon to be diffusely transmitted through an opaque slab. The experimental setup consists of a Coherent Compass 315M-100 laser emitting 532 nm light, followed by the polycarbonate foam cell and a photocell for the detection of the diffusely transmitted photons. As foams coarsen by gas diffusion from smaller to larger bubbles, the transmitted intensity increases. Coarsening is a self-similar process, and the time dependence of the transmitted intensity can be fit to the form  $I(t) = I_0(1 + t/t_0)^{1/2}$ , where  $I_0$  is the initial intensity and  $t_0$  is related to the coarsening rate [13]. We extract  $I_0$  from our transmission data and normalize it with the diffuse intensity transmitted through a reference polyball sample (monodisperse polystyrene spheres of size = 93 nm, thickness of sample = 4 mm,  $l^* = 0.5 \text{ mm}$ ) to obtain the diffuse transmission probability  $T_d$ .

To relate  $T_d$  data to transport parameters, we use the prediction of ref. [14],

$$T_d = \frac{1 + z_e}{[1 + (D_0^2 + z_e^2)\mu'_a/D_0] \sinh[L'\sqrt{\alpha}]/\sqrt{\alpha} + 2z_e \cosh[L'\sqrt{\alpha}]}. \quad (3)$$

Here  $z_e$  is the extrapolation length ratio, whose value ranges between 0.9 and 1.8 according to liquid fraction [8];  $L' = L/l^*$  is the dimensionless slab thickness;  $D_0 = 1/3$  is the dimensionless

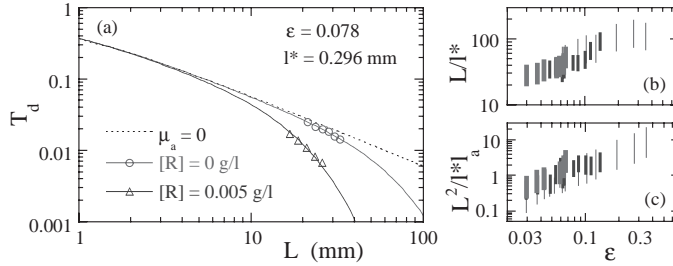


Fig. 1 – (a) Transmission *vs.* slab thickness for example foams of liquid fraction  $\epsilon = 0.78$ , both without rhodamine (circles) and with rhodamine dye of concentration  $[R] = 0.005$  g/l (triangles). The solid curves show fits to eq. (3), giving  $l^* = 0.296$  mm and  $\mu_a' = 3 \times 10^{-5}$  for  $[R] = 0$  g/l and giving  $\mu_a' = 4.270 \times 10^{-4}$  ( $l_a = 693$  mm) for  $[R] = 0.005$  g/l. The dashed line shows the expectation with no absorption whatsoever. Plots (b) and (c) show the figures of merit for all experiments:  $[R] = 0.005$  g/l (thin),  $[R] = 0.01$  g/l (medium) and  $[R] = 0.012$  g/l (thick). Error bars in both plots are roughly ten percent.

diffusion coefficient in three dimensions;  $\mu_a' = l^*/l_a$  indicates the strength of absorption; and  $\alpha = \mu_a'(1/D_0 + \mu_a')$ . With no absorption,  $T_d$  goes roughly as  $l^*/L$ ; correspondingly, a typical transmitted photon experiences  $(L/l^*)^2$  scattering events, and has a path length of  $L^2/l^*$ . Absorption is therefore appreciable if  $L^2/l^*$  is comparable to  $l_a$ . Figures of merit for the importance of scattering and absorption are thus, respectively,  $L/l^*$  and  $L^2/(l^* l_a)$ .

To accurately extract  $l_a$ , it is crucial to have an accurate value of  $l^*$ . Our strategy is to compare pairs of foam samples that are identical, except for the presence/absence of dye. Example transmission data for such a pair are shown in fig. 1a, as a function of slab thickness. Best fits to eq. (3) are also included. For the sample without dye, both  $l^*$  and  $l_a$  are adjusted; the latter is included since there is some slight absorption by the surfactant solution. Results for  $l^*$  are consistent with eq. (1). For the sample with dye, the value of  $l^*$  is now fixed and the only adjustable parameter is  $l_a$ . For both, good fits are obtained with no adjustment to the overall normalization. This same procedure is used for foams with different liquid fractions, and for three different dye concentrations:  $[R] = \{0.0050 \text{ g/l}, 0.0100 \text{ g/l}, 0.0124 \text{ g/l}\}$ . The figures of merit for scattering and absorption for all samples, plotted in figs. 1b-c, demonstrate that we are within the limits of the validity of eq. (3). Specifically,  $L$  and  $l_a$  are safely greater than  $5l^*$ ; furthermore,  $l_a$  is within an order of magnitude of the typical path length, giving a level of absorption that is detectable but not overwhelming.

**Results.** – Diffuse transmission data are collected and analyzed, per above, for the absorption lengths of the foams. The results are divided by the known absorption length of the solution, and plotted in fig. 2 as a function of liquid fraction. The same trends are displayed by the samples made with the three different dye concentrations. Namely, the foams are far less absorptive than the solutions (*e.g.*, clear red liquid produces opaque pink foam). Quantitatively, at both low and high liquid fractions, the value of  $l_a/l_a^{\text{soln}}$  is consistent with  $1/\epsilon$ . Therefore, according to eq. (2), the photons execute a perfectly random walk in these samples. By contrast, for foams of intermediate wetness  $0.04 < \epsilon < 0.2$ , the ratio  $l_a/l_a^{\text{soln}}$  falls below  $1/\epsilon$ . Therefore, according to eq. (2), the fraction  $f$  of a photon path that lies in the liquid is greater than  $\epsilon$ . For these samples, the photon paths are not random but instead preferentially lie in the liquid phase.

One possible explanation is that photons are trapped within the long, thin Plateau borders by total internal reflection, just as happens in an optical fiber. This effect is largest at  $\epsilon \approx 0.07$ ,

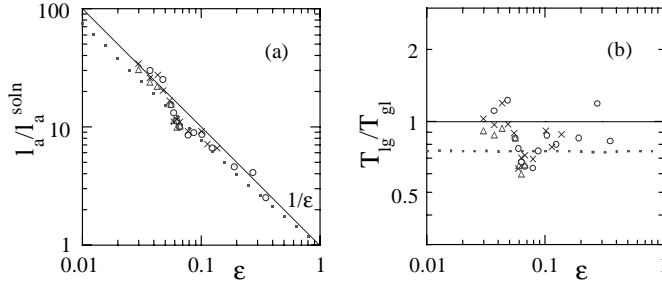


Fig. 2 – Foam absorption length (a), and average interface transmission ratio (b), *vs.* liquid fraction for foaming solutions with rhodamine concentrations  $[R] = 0.005$  g/l (circles), 0.01 g/l (crosses), and 0.012 g/l (triangles). The solid lines are  $l_a/l_a^{\text{soln}} = 1/\epsilon$  and  $T_{lg}/T_{gl} = 1$ , which correspond to diffuse photon propagation by a completely random walk. The small points represent simulation results.

with a value of  $l_a/l_a^{\text{soln}}$  indicating that paths are trapped in the borders about 40 percent more than for a perfectly random walk. In wetter foams, the trapping effect vanishes and the paths are random, perhaps because the Plateau borders become short and thick (they vanish altogether at  $\epsilon \approx 0.36$ , where the bubbles are randomly close-packed spheres). For drier foams, the trapping effect also vanishes, perhaps because the vertices are so small and sharp that trapped photons rarely cannot turn the corner from one border to another.

To quantify our intuition regarding total internal reflection, we now connect our data for  $l_a/l_a^{\text{soln}} = 1/f$  *vs.*  $\epsilon$  to the average transmission probabilities for photons going from liquid to gas,  $T_{lg}$ , and for photons going from gas to liquid,  $T_{gl}$ . The first step is to write down continuity conditions for the photon concentration per unit volume,  $\rho_i$ , and per unit length along an actual path,  $\lambda_i$ , in each phase  $i$ . Since photon speed varies with the refractive index  $n$ , one condition is that  $\lambda_i/n_i$  be constant. Next, since the rate at which photons enter and exit each phase must be the same, the other requirement is that  $(\rho_i/n_i)T_{ij}$  be constant. These two conditions may be used separately to compute the fraction of photons in each phase, the former in terms of  $f$  and the latter in terms of  $\epsilon$ . Equating the two gives

$$\frac{T_{lg}}{T_{gl}} = \frac{\epsilon(1-f)}{f(1-\epsilon)}. \quad (4)$$

Note that for random walk scattering ( $f = \epsilon$ ), the expected result ( $T_{lg} = T_{gl}$ ) is obtained.

Using eq. (4) and the data of fig. 2(a), we compute the transmission probability ratios for all our samples and plot the results *vs.*  $\epsilon$  in fig. 2(b). At high and low liquid fractions, where  $f \approx \epsilon$ , we find  $T_{lg} \approx T_{gl}$ . At intermediate liquid fractions, where  $f > \epsilon$ , we find  $T_{lg} < T_{gl}$ . Therefore, photons in the liquid are more likely to reflect when striking a gas interface than vice versa. This is consistent with the notion of trapping by total internal reflection.

*Simulation.* – To further investigate photon channelling, we simulate transport in a two-dimensional foam crystal. The elementary unit is a hexagon, with the boundary decorated by liquid according to the desired liquid fraction. To mimic three-dimensional foam structure, the edge thickness  $t$  and the radius of curvature of the vertices  $R$  have a constant ratio. For the example of fig. 3, we chose  $R = 2t$ ; identical results were found for  $R = 1000t$ . By symmetry, it is enough to confine photons to a  $30^\circ$ – $60^\circ$ – $90^\circ$  triangle as sketched in fig. 3. They reflect with unit probability when striking the boundary of the confining triangle; they reflect or refract probabilistically according to the Fresnel and Snell laws when striking the gas/liquid interface. The initial position is taken at random. The initial direction is nearly random; we

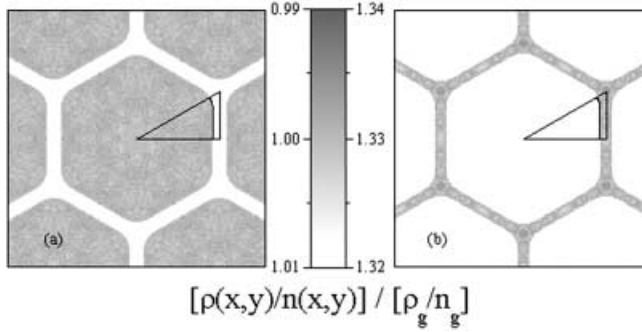


Fig. 3 – Simulation results for photon density *vs.* position, normalized by the average value in the gas phase, in an idealized structure with liquid fraction  $\varepsilon = 0.15$ ; photons are actually confined to the triangle, which is then used to tile the rest of space. In the absence of channelling, for truly random walks,  $\rho/n$  would be constant.

exclude initial angles close to integer multiples of  $30^\circ$ , since these take inordinately long to randomize [11].

To see channelling directly, first we measure the optical density of photons  $\rho(x, y)/n(x, y)$  *vs.* position  $(x, y)$ . In the absence of channelling, this quantity is constant throughout the whole area of the foam. Example grey scale plots of optical density for  $\varepsilon = 0.15$  are shown in fig. 3. This figure is based on 1000 photons, each traveling for an average distance of 16000 bubble edge lengths. This degree of statistics is sufficient to demonstrate an excess optical density of photons in the liquid phase by a factor of about 1.33 times the optical density of the gas phase. Just as in experiment, the simulated photons stay in the liquid more than if their trajectories were truly random walks. As an aside, the optical density appears to be uniform in the gas phase but exhibits some fine structure in the liquid phase. However, it varies from run to run and so is likely due to limited statistics in the simulation.

In order to compare simulation with experiment, and to rigorously check the simulation, we compute the transmission ratio  $T_{lg}/T_{gl}$  in three different ways. The first is by averaging the optical density over each phase and using the continuity condition,  $T_{lg}/T_{gl} = (\rho_g/n_g)/(\rho_l/n_l)$ . The second is by literally averaging the two transmission probabilities over all interface encounters. The third is by finding the total path length  $L$  and length in solution  $L^{\text{soln}}$ , and using  $L/L^{\text{soln}} = l_a/l_a^{\text{soln}} = 1/f$  along with eq. (4). Typically, the latter two methods are done for 100 photons each travelling an average distance of 17000 bubble edge lengths.

The three methods give indistinguishable results. Namely, the transmission ratio appears to be constant, independent of liquid fraction, as shown by the small symbols in fig. 2(b). The average optical density ratio in fig. 3, combined with the continuity condition, gives  $T_{lg}/T_{gl} = 0.7501 \pm 0.0001$ , where the uncertainty is based on the standard deviation divided by the square root of the number of pixels. Methods two and three give  $0.749 \pm 0.003$  and  $0.751 \pm 0.005$ , respectively, where the uncertainties are the standard deviation of the values at different liquid fractions. All are consistent with  $T_{lg}/T_{gl} = 0.75$ , which corresponds to  $l_a/l_a^{\text{soln}} = 0.75/\varepsilon + 0.25$ , according to eqs. (2), (4). Thus, the simulation agrees quite well with experiment, but only where the channelling effect is strong. At high and low liquid fractions, channelling ceases in experiment but not in simulation. Perhaps this is due to the two-dimensional nature of the simulation, or to the neglect of disorder and thin-film interference effects. Curiously, the simulated transmission ratio is consistent with  $T_{lg}/T_{gl} = n_g/n_l$ ; this is also supported by additional simulations for different  $n_l$  values.

*Conclusion.* – To first approximation, foams absorb light according to the absorptivity and volume fraction of the liquid solution. However, many foams ( $0.04 < \varepsilon < 0.2$ ) exhibit up to about 40% more absorption than this simplest expectation. Evidently, photon paths sample the liquid phase up to about 40% more than for a truly random walk. Intuitively, photons are channelled along the Plateau borders, much like the trapping of photons in an optical fiber by total internal reflection. A similar guiding of photons is exploited in certain plant and animal cells [15]. Our conclusion is supported by data on foams made from three different absorbing solutions, as well as by simulations of transport in an idealized structure. At long length scales, larger than the bubble size, the photon propagation may be described by a diffusion coefficient. However at short length scales, comparable to the bubble size, the diffusion approximation apparently fails since the photon concentration field is not homogeneous. The step sizes in a photon's random walk have a well-defined average ( $l^*$ ), but are not randomly drawn from an exponential distribution. Rather, the steps must be correlated with local structure, being longer when in the gas and shorter when in the liquid. And the propagation direction may be correlated with the local foam microstructure as well, for instance aligned with the Plateau borders. This, and the role played by vertices [10] and films [11], beg for complete theoretical understanding. Not only would we more clearly understand why seemingly black liquids like Guinness Stout produce rich brown foams, but we would also more fully be able to exploit diffusing light spectroscopies.

\* \* \*

We thank S. SKIPETROV and H. STARK for sharing their results. Our work was supported by NASA Microgravity Fluid Physics grant NAG3-2481.

## REFERENCES

- [1] WEAIRE D. and HUTZLER S., *The Physics of Foams* (Oxford University Press, New York) 1999.
- [2] DURIAN D. J., WEITZ D. A. and PINE D. J., *Science*, **252** (1991) 686.
- [3] EARNSHAW J. C. and JAAFAR A. H., *Phys. Rev. E*, **49** (1994) 5408.
- [4] COHEN-ADDAD S. and HOHLER R., *Phys. Rev. Lett.*, **86** (2001) 4700.
- [5] KAPLAN P. D., DINSMORE A. D., YODH A. G. and PINE D. J., *Phys. Rev. E*, **50** (1994) 4827.
- [6] WEITZ D. A. and PINE D. J., *Dynamic Light Scattering: The Method and Some Applications*, edited by BROWN W. (Clarendon, Oxford) 1993, p. 652.
- [7] MARET G., *Curr. Opin. Colloid Interface Sci.*, **2** (1997) 251.
- [8] VERA M. U., SAINT-JALMES A. and DURIAN D. J., *Appl. Opt.*, **40** (2001) 4210.
- [9] KOEHLER S. A., HILGENFELDT S. and STONE H. A., *Langmuir*, **16** (2000) 6327.
- [10] SKIPETROV S., unpublished (2002).
- [11] MIRI M. and STARK H., *Phys. Rev. E*, **68** (2003) 031102.
- [12] SAINT-JALMES A., VERA M. U. and DURIAN D. J., *Eur. Phys. J. B*, **12** (1999) 67.
- [13] VERA M. U. and DURIAN D. J., *Phys. Rev. Lett.*, **88** (2002) 88304.
- [14] COX A. A. and DURIAN D. J., *Appl. Opt.*, **40** (2001) 4228.
- [15] LAKSHMINARAYANAN V. and ENOCH J. M., *Handbook of Optics*, 2nd edition, Vol. **III**, edited by BASS M. (McGraw-Hill, New York) 2001, pp. 9.1-31.